



"HENRI COANDA"
AIR FORCE ACADEMY
ROMANIA



"GENERAL M.R. STEFANIK"
ARMED FORCES ACADEMY
SLOVAK REPUBLIC

INTERNATIONAL CONFERENCE of SCIENTIFIC PAPER
AFASES 2015
Brasov, 28-30 May 2015

AERODYNAMIC CHARACTERISTICS OF AIRFOIL WITH SINGLE SLOTTED FLAP FOR LIGHT AIRPLANE WING

Michael Damianov Todorov*

*Faculty of Transport, Technical University of Sofia, Bulgaria

Abstract: A numerical study was performed on a NACA 23012 airfoil with a single slotted flap to examine the aerodynamic coefficients at Reynolds number of 3×10^6 , and for help to identifying the forces acting on a light airplane wing. Besides, in the paper the flow fields around the airfoil with single slotted flap were shown. All calculations were made using a CFD code Fluent. For a turbulent model the Spalart-Allmaras method was chosen. Conclusions were made about the aerodynamic efficiency of the proposed configuration wing-single slotted flap.

Keywords: airplane wing, single slotted flap, aerodynamic characteristics, CFD, Fluent

1. INTRODUCTION

Aircraft wing high-lift configuration design is an important and challenging part of the whole aircraft aerodynamic configuration design, even dealing with a 2-D high-lift configuration design task which is an essential step for the 3-D high-lift configuration design [10], [12], [13].

During the take-off and landing of an aircraft, the performance of high-lift devices has strong impact on the operating costs and environment around airports, such as improvements of payload, fuel consumption, and noise emission. Take-off and landing performance for very light airplanes are governed by the requirements as EASA CS-VLA [5]. The take-off and landing distances, and the important speeds as the stall speed with flaps retracted – V_S , the design maneuvering speed – V_A , the speed with flaps fully deflected – V_F , and the stall speed with flaps fully deflected – V_{SF} , depend on aerodynamic

characteristics of the wing with a flaps deflected.

Nowadays, Computational Fluid Dynamics (CFD) is widely used for the prediction of the aerodynamic performance of the wing, at least in cruise flight. The computation of the flow over a multi-element wing in high-lift configuration remains however one of the most difficult problems encountered in CFD [3]. The computations normally include a comprehensive code, coupled to Euler or Navier-Stokes solvers. The examples for a successful application of CFD are the codes FLUENT, OVERFLOW of NASA, FLOWer and TAU of Deutsches Zentrum für Luft und Raumfahrt [3], [12], elsA and WAVES of ONERA [6], CFD++ [15], Star-CCM+ [11], [8], TAS of Takoku University and UPACS of Japan Institute of Space Technology and Aeronautics [7, 8].

The high-lift configurations considerably complicate the flow physics by boundary layer transition, separations and reattachments.

Therefore it is very important to generate the appropriate mesh around it. The mesh can be structured, unstructured or hybrid. The structured mesh is identified by regular connectivity. The possible element choices are quadrilateral in 2D and hexahedral in 3D. This model is highly space efficient, i.e. since the neighborhood relationships are defined by storage arrangement. Some other advantages of structured mesh are better convergence and higher resolution. But obviously it cannot be used for very complicated geometry. The unstructured mesh is identified by irregular connectivity, [6], [9]. It cannot easily be expressed as a two-dimensional or three-dimensional array. This allows the usage of a solver for any possible element. Compared to structured meshes, this model can be highly space inefficient since it calls for explicit storage of neighborhood relationships. These grids typically employ triangles in 2D and tetrahedral in 3D. A hybrid mesh contains a mixture of structured portions and unstructured portions. It integrates the structured meshes and the unstructured meshes in an efficient manner, [12].

Another important step is the choice of a turbulent model. The turbulence is the most challenging area in fluid dynamics and the most limiting factor in accurate computer simulation of the flow. An overview of turbulence modeling is done in [2]. There are the following turbulent models, [16]:

- The *direct numerical simulation* (DNS) of Navier-Stokes equation can be applied only for very low Reynolds numbers and very simple and limited geometries, and practically no numerical solution for flows of interest to engineers can be obtained.

- *Large eddy simulation* (LES) solves the spatially averaged Navier-Stokes equations. Large eddies are directly resolved, but eddies smaller than the mesh are modeled. LES is less expensive than DNS, but the amount of computational resources and efforts are still too large for most practical applications.

- *Spalart-Allmaras* is a low-cost Reynolds-Averaged Navier-Stokes (RANS) model solving a transport equation for a modified eddy viscosity. It is designed specifically for aerospace applications involving wall-bounded flows. It embodies a

relatively new class of one-equation models where it is not necessary to calculate a length scale related to the local shear layer thickness.

- The $k-\epsilon$ *turbulent models* are the most widely-used engineering turbulence model for industrial applications, which are a robust and a reasonably accurate. However they generally perform poorly for flows with strong separation, large streamline curvature, and large pressure gradient.

- The $k-\omega$ *turbulence models* have gained popularity mainly because the model equations do not contain terms which are undefined at the wall, i.e. they can be integrated to the wall without using wall functions, and they are accurate and robust for a wide range of boundary layer flows with pressure gradient. Reynolds stresses are solved directly using transport equations, avoiding isotropic viscosity assumption of other models. It is used for highly swirling flows. The quadratic pressure-strain option improves performance for many basic shear flows.

In [14], it was found the aerodynamic characteristics of an airfoil with single plain flap, as it is shown in Fig.1. For this purpose, first it was obtained numerical results for NACA 23012 airfoil which were compared with experimental wind tunnel data [1] to select density mesh and turbulent model. The aerodynamic characteristic were obtained by commercial CFD code FLUENT. It was generated structured mesh. The Spalart-Allmaras method gave closest results to the experimental data.

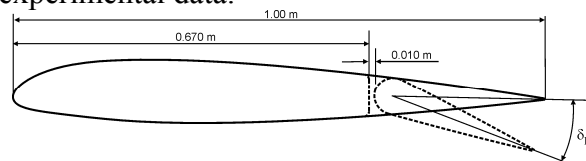


Figure 1. *NACA 23012 airfoil with single plain flap* [14]

Then the aerodynamic characteristics of NACA 23012 airfoil with single flap were calculated. It was generated multi-object hybrid mesh. The calculations were made for Reynolds number of $Re=3 \times 10^6$ (respectively $V=43.81$ m/s) at the sea level. The turbulent intensity and turbulent viscosity were 2.48% and 10 respectively. The flap deflection angle, δ_F , was 20° .



"HENRI COANDA"
AIR FORCE ACADEMY
ROMANIA



"GENERAL M.R. STEFANIK"
ARMED FORCES ACADEMY
SLOVAK REPUBLIC

INTERNATIONAL CONFERENCE of SCIENTIFIC PAPER
AFASES 2015
Brasov, 28-30 May 2015

The obtained results show that the chosen arrangement of wing-single plan flap is not sufficiently effective from an aerodynamic point of view, although it is attractive with the simple design.

Therefore, in the proposed paper another configuration will be studied: an airfoil with a single slotted flap, as it is outlined in Fig.2. A NACA 23012 airfoil with a 1.00 m chord has been used in all the CFD simulations. The single slotted flap with a 0.32 m chord, corresponding to 32% chord, has been constructed in such a way as to match the geometry of the baseline airfoil.

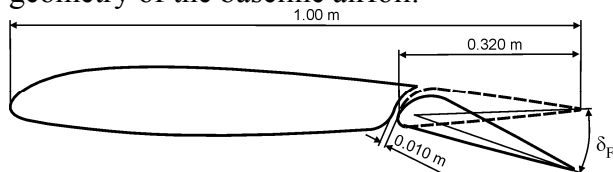


Figure 2. NACA 23012 airfoil with single slotted flap

2. AERODYNAMIC CHARACTERISTICS OF NACA 23012 AIRFOIL WITH A SINGLE SLOTTED FLAP

To calculate the aerodynamic characteristics of NACA 23012 airfoil with a single slotted flap, the multi-object hybrid O-mesh is generated. The circle has a $10c$ (c -airfoil chord) radius. Around the airfoil, the flap and downstream are provided with a high refinement, as it is shown in Fig.3. Thus the mesh has 711 754 nodes and 706 558 elements.

The calculations are made for Reynolds number of $Re=3 \times 10^6$ (respectively $V=43.81$ m/s) at the sea level. The turbulent intensity and turbulent viscosity are 2.48% and 10 respectively. The flap deflection angle, δ_F , is 20° .

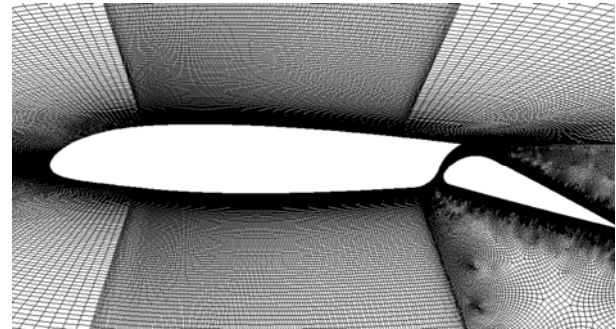


Figure 3. View of the mesh geometry of NACA 23012 airfoil with single slotted flap

Fig.4 and Fig.5 show $C_L-\alpha$ and $C_D-\alpha$ data of the numerical results for a NACA 23012 airfoil, NACA 23012 airfoil with a single plain flap, and NACA 23012 airfoil with a single slotted flap.

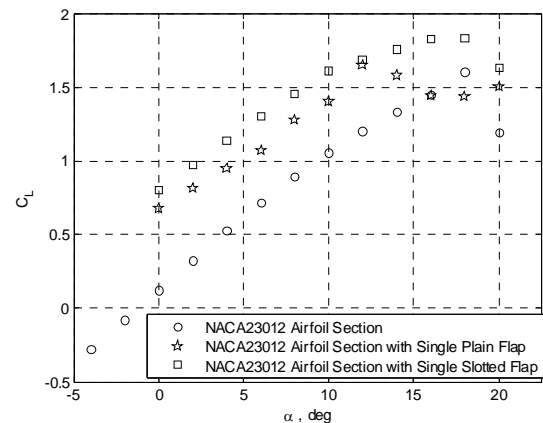


Figure 4. Lift coefficient C_L plot over the range of angles of attack of the numerical results for a NACA 23012 airfoil, NACA 23012 airfoil with a single plain flap, and NACA 23012 airfoil with a single slotted flap

Figures 6, 7, and 8 show pressure coefficients, pressure, and velocity fields around NACA 23012 airfoil with a single slotted flap in the range from 0° to 20° angles of attack.

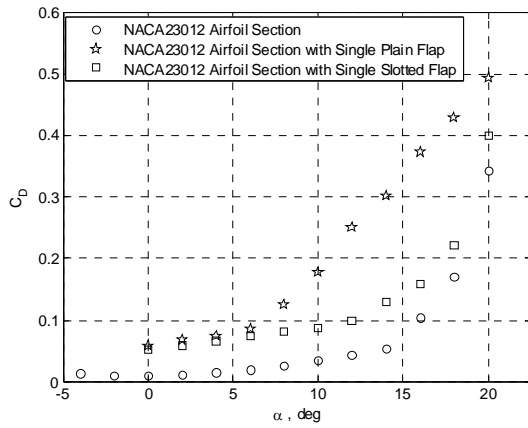


Figure 5. Drag coefficient C_D plot over the range of angles of attack of the numerical results for a NACA 23012 airfoil, NACA 23012 airfoil with a single plain flap, and NACA 23012 airfoil with a single slotted flap

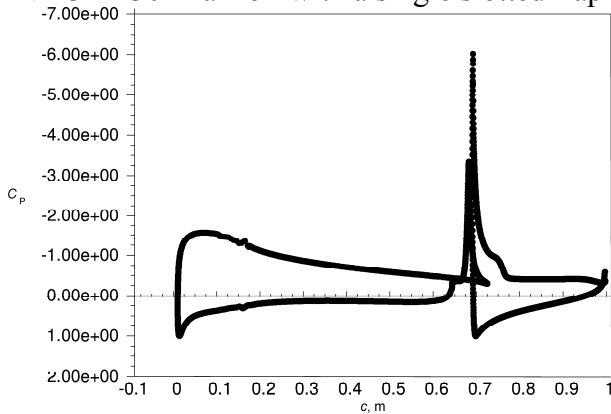


Figure 6a. Pressure coefficient of NACA 23012 airfoil with a single slotted flap at $\alpha=2^\circ$

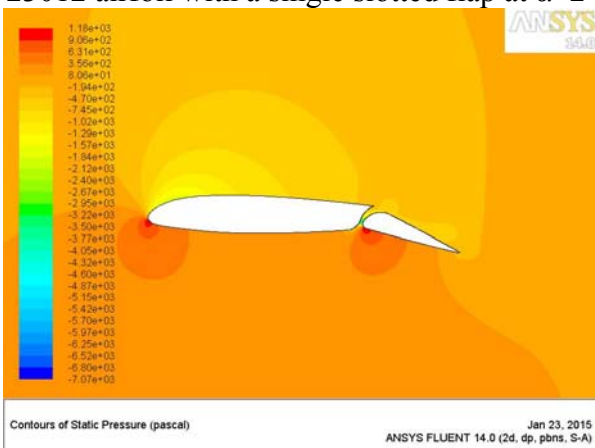


Figure 6b. Pressure around NACA 23012 airfoil with a single slotted flap at $\alpha=2^\circ$

3. DISCUSSION

The deflection of the single slotted flap results in an increase in the lift coefficient by about 38% compared to the baseline airfoil, in the range of angles of attacks from 0 to 10° (see Fig.4).

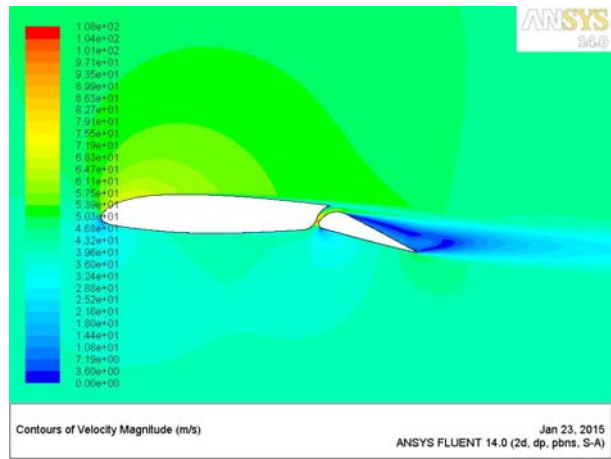


Figure 6c. Velocity fields around NACA 23012 airfoil with a single slotted flap at $\alpha=2^\circ$

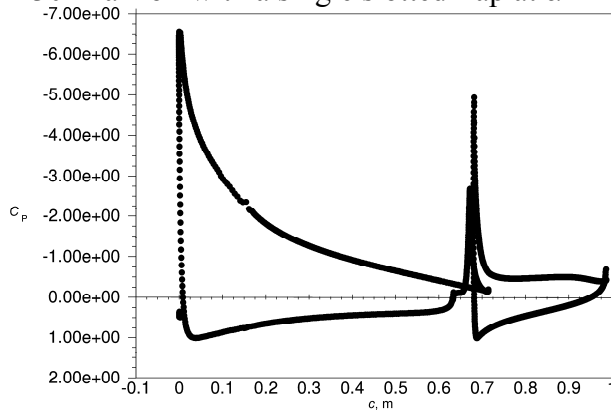


Figure 7a. Pressure coefficient of NACA 23012 airfoil with a single slotted flap at $\alpha=12^\circ$

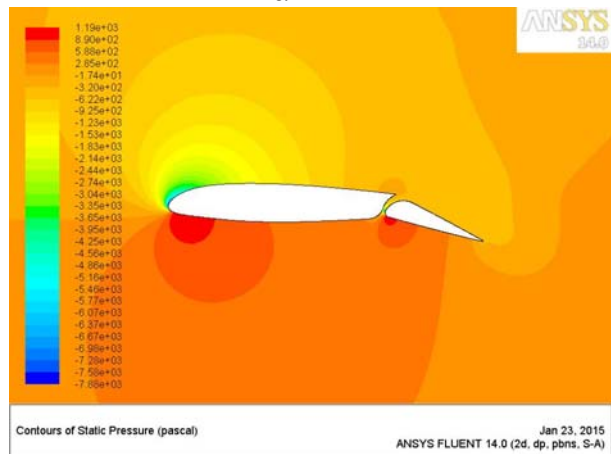


Figure 7b. Pressure around NACA 23012 airfoil with a single slotted flap at $\alpha=12^\circ$

This is about 8% higher lift coefficient than of the configuration with the single plain flap.



"HENRI COANDA"
AIR FORCE ACADEMY
ROMANIA



"GENERAL M.R. STEFANIK"
ARMED FORCES ACADEMY
SLOVAK REPUBLIC

INTERNATIONAL CONFERENCE of SCIENTIFIC PAPER
AFASES 2015
Brasov, 28-30 May 2015

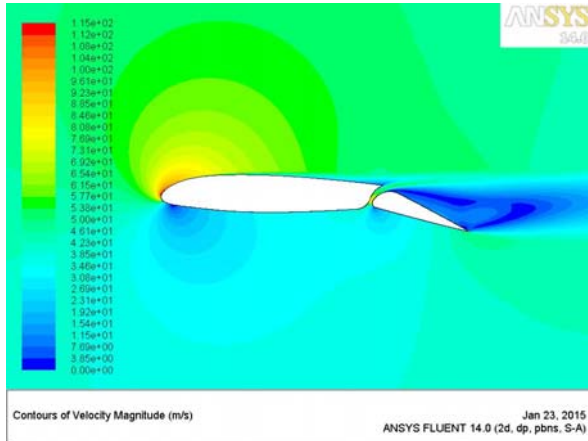


Figure 7c. Velocity fields around NACA 23012 airfoil with a single slotted flap at $\alpha=12^\circ$

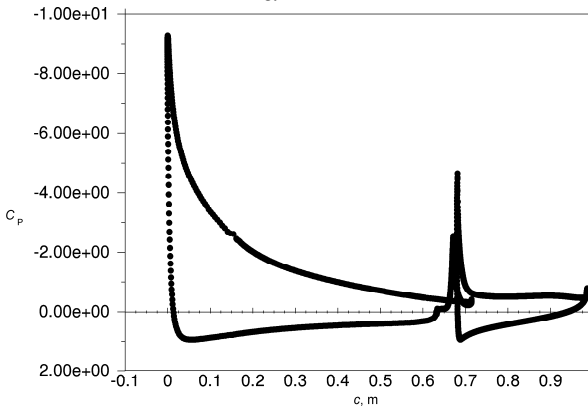


Figure 8a. Pressure coefficient of NACA 23012 airfoil with a single slotted flap at $\alpha=18^\circ$

The maximum angle of attack in the case with a deflected single slotted flap is 18° . The maximum angle of attack of the baseline airfoil is the same, while in the case with the wing with a single plain flap it is 12° . This is because after $\alpha=12^\circ$ the flow is fully detached to the upper surface, as it is shown in [14]. The bigger lift coefficient is due to the gap between the flap and the wing, and the selected geometry of the lower surface at the end of the wing airfoil.

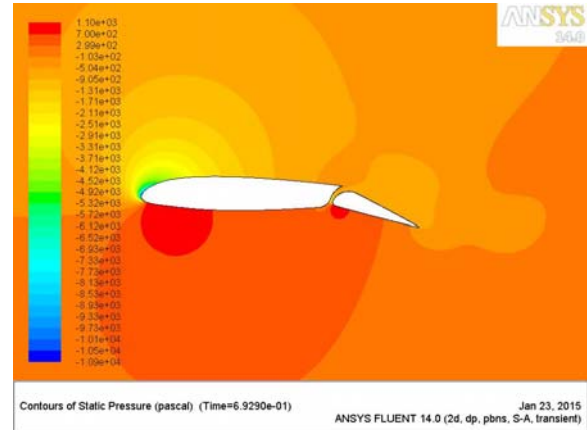


Figure 8b. Pressure around NACA 23012 airfoil with a single slotted flap at $\alpha=18^\circ$

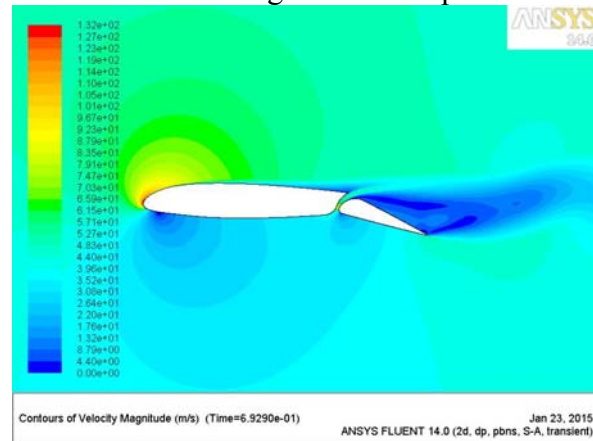


Figure 8c. Velocity fields around NACA 23012 airfoil with a single slotted flap at $\alpha=18^\circ$

They force high pressure air from below the wing over the flap helping the airflow to remain attached to the flap.

The deflection of the single slotted flap increases the drag coefficient at the high angles of attack less than the configuration with single plain flap. This is favorable since the flap is used in this configuration for take-off, i.e. at high angles of attack.

These results show that the chosen arrangement of a wing-single slotted flap is more effective than the configuration wing-single plain flap.

4. CONCLUSIONS

A numerical analysis was performed for a NACA 23012 airfoil with a single slotted flap. All calculations were performed with the Fluent code. It was used the Spalart-Allmaras turbulent method.

The analysis aimed to identify the aerodynamic forces acting on the proposed wing and flap at Reynolds number of 3×10^6 .

The 2D CFD model was used to examine the major features around the proposed configuration wing-single slotted flap.

The obtained results were compared with those for the NACA 23012 baseline airfoil and configuration wing- single plain flap.

The CFD results for the proposed configuration wing-single slotted flap showed higher lift coefficient than the NACA 23012 baseline airfoil and configuration wing-single plain flap. The drag coefficient is less than that of the configuration wing-single plain flap. The obtained results are better from the aerodynamic point of view.

The further work is needed to investigate the influence of the gap and position of axis of rotation of the single slotted flap to improve of the aerodynamic characteristics of designed configuration airfoil-flap.

REFERENCES

1. Abbott, I. H., von Doenhoff, A. E.. Summary of airfoil data, *NACA Report No. 824*, (1945).
2. Anderson, B., Anderson, R., Hakanson, L., Mortensen, L., Sudiyo, R., van Wachem, B.. Computation fluid dynamics for engineers, *Cambridge University Press*, (2012).
3. Brezillon, J., Dwight, R. P., Wild, J.. Numerical aerodynamic optimization of 3D high-lift configuration, *Proc. of 26th International Congress of The Aeronautical Sciences, ICAS* (2008).
4. van Dam, C.P.. The aerodynamic design of multi-element high-lift systems for transport airplanes, *Progress on Aerospace Sciences*, 38, 101-144, (2002).
5. EASA, Certification specifications for very light aeroplanes CS-VLA, Amendment 1, (March 2009).
6. Khare, A., Baig, R., Ranjan, R., Shah, S., Pavithran S., Moitra, A.. Computational simulation of flow over a high-lift trapezoidal wing, *Proc. of ICEAE* (2009).
7. Murayama, M., Yamamoto, K., Numerical simulation of high-lift configurations using unstructured mesh method, *Proc. Of 24th International Congress of The Aeronautical Sciences, ICAS* (2004).
8. Murayama, M., Yokokawa, Y., Yamamoto, K.. Validation study of CFD analysis for high-lift systems, *Proc. Of 25th International Congress of The Aeronautical Sciences, ICAS* (2006).
9. de Oliveira Neto, J. A., Cavali, D., Junior, C. B., Azavedo J.L.F., de Lima e Silva, A. L. F.. Computational simulations of high-lift configuration using unstructured grids, *Proceedings of the ENCIT 2006*, ABCM, Curitiba – PR, Brazil – Paper CIT06-0269 (2006).
10. Prabhar, A., Ohri, A.. CFD analysis on MAV NACA 2412 wing in high lift take-off configuration for enhanced lift generation, *J. Aeronautics & Aerospace Engineering*, volume 2, 1-8, issue 5, (2013).
11. Shankara, P., Snyder, D., Numerical simulation of high lift trap wing using STAR-CCM+, *AIAA 2012-2920*, (2012).
12. Schindler, K., Reckzech, D., Scholz, U., Aerodynamic design of high-lift devices for civil transport aircraft using RANS CFD, *AIAA 2010-4946*, (2010).
13. Steed, R. G. F.. High lift CFD simulation with an SST-based predictive laminar to turbulent transition model, *AIAA 2011-864*, (2011).
14. Todorov, M., Aerodynamic Characteristics of Airfoil with Single Plain Flap for Light Airplane Wing, *Proc. of ICMT*, (2015).
15. Vecchia, P. D., Ciliberty, D.. Numerical aerodynamic analysis on a trapezoidal wing with high lift devices: a comparison with experimental data, *XXII AIDAA Conference*, (2013).
16. www.fluentusers.com